
STRUCTURE, PHASE TRANSFORMATIONS,
AND DIFFUSION

Effects of Reciprocating Speed on Corrosive Wear Behavior of Cold-Sprayed Al Coating on Offshore Platforms

Zhang Jing^{a,b} and Kong Dejun^{a,*}

^a*College of Mechanical Engineering, Changzhou University, Changzhou, 213164 P.R. China*

^b*School of Mechanical Engineering, Donghua University, Shanghai, 201620 P.R. China*

**e-mail: kong-dejun@163.com*

Received August 25, 2019; revised October 16, 2019; accepted November 27, 2019

Abstract—An Al coating was fabricated on S355 structural steel using a cold spraying. The morphologies, chemical composition and phases of obtained coating were analyzed using a field emission scanning electronic microscope (FESEM), energy dispersive spectrometer (EDS), and X-ray diffraction (XRD), respectively. The cold sprayed Al coating was conducted to simulate the friction-wear behavior in 3.5% NaCl solution. The results show that the average coefficients of friction (COFs) of cold sprayed Al coating at the reciprocating speeds of 5, 6.67 and 8.33 Hz are 0.29, 0.28, and 0.24, respectively, which decrease with the increase of reciprocating speed, the Al coating has the excellent performance of friction reduction. The wear mechanisms of Al coating at the reciprocating speeds of 5, 6.67 and 8.33 Hz are abrasive wear, fatigue wear and corrosive wear.

Keywords: cold spraying, Al coating, corrosive wear, coefficient of friction (COF), wear mechanism, corrosion resistance

DOI: 10.1134/S0031918X20130207

INTRODUCTION

S355 steel with the high plasticity and impact toughness is used in the environment of salt spraying corrosion (SSC) [1], humidity, seawater, and etc., which is corroded by the corrosive ions in marine environment. At the same time, the corrosive wear easily occurs in seawater with the sand and gravel, which greatly impairs the mechanical performance of S355 steel and further influences the safety on offshore platforms [2]. Al is more easily to loss electronic than Fe to provide cathodic protection for the substrate [3], which is used as the protection on offshore platforms, Al coating with high bonding strength and low brittleness can effectively prevent the occurrences of cracking, foaming, rusting and shedding, which exhibits high corrosion resistance than Zn coating. Thermal sprayed Al coating is a main method of protecting S355 steel, traditional thermal sprayed coatings have some disadvantages such as high residual stress, thermal defects, poor binding force, and etc. [4–6], resulting in fast corrosion of Al coating, the corrosion products generate the bubble phenomenon to lead to the failure of Al coating.

As a new spraying technology, cold spraying processes the advantage of supersonic gas with the critical speed to impact the substrate, the metal powders are bonded with the substrate [7–9]. The thermal softening exceeds the adiabatic shearing instability (ASI) of

strain hardening, which is the mechanism of cold spraying deformation [10–13]. Compared with thermal spraying, the cold sprayed Al coating has low residual stress and little porosity, which improved its corrosion resistance [14, 15]. Morgan et al. [16] and Li et al. [17] investigated the forming mechanism, surface morphology and bonding capacity of cold sprayed Al coating; Bai et al. [18] analyzed the corrosion performance of cold sprayed Al–Al₂O₃ coatings on mild carbon steel under thermal insulation; and Assadi et al. [19] analyzed the effects of coating defects on the corrosion behavior of cold sprayed refractory metals. However, there are few reports on the corrosive wear performance of Al coating in seawater.

In this study, an Al coating was fabricated on S355 structural steel using a cold spraying. The aim was to investigate the effects of reciprocating speed on the friction-wear performance of Al coating in 3.5% NaCl solution, which provided an experimental basis for the application of cold sprayed Al coating in marine environment.

EXPERIMENTAL

Fabrication of Samples

The experimental substrate was European standard S355 structural steel with the chemical component (wt %): C 0.17, Si 0.55, Mn 0.94, P 0.035, Cr 0.065,

S 0.035, Ni 0.065, Mo 0.30 and Zr 0.15, the rest was Fe. The cold spraying process: mechanical polishing → chemical washing to remove oil → rust removal → rinsing and drying → cold sprayed Al coating → cooling → cleaning surface. The Al particle with the diameter of 20–45 μm was used as cold sprayed powder, the cold spraying test was performed on a Kinetiks 4000 type cold spraying equipment, technological parameters: pressure of 3.5 MPa, temperature of 400°C, spraying distance of 40 mm, gun speed of 200 m/s, powder feeding speed of 1 L/min. After the cold spraying, the obtained Al coating was sealed using a DIAMANT Dichtol WFT (1532) type sealing agent.

Characterization Methods

The morphologies of obtained Al coating surface and cross-section were observed using a SUPRA-55 type field emission scanning electronic microscope (FESEM) and energy dispersive spectrometer (EDS), respectively, its phases were determined using a D/max2500 PC type X-ray diffractometer (XRD), and the hardness of Al coating was measured using a HMV-2T micro-hardness tester. The friction-wear test was carried out on a CFT-I type friction-wear tester.

The Al coating was immersed in 3.5% NaCl solution to investigate the effects of reciprocating speed on the corrosive friction-wear behavior of Al coating, test parameters: friction-pair of Si_3N_4 ceramic ball with the diameter of 3.5 mm, wear length of 5 mm, Wear time of 2 h, respective reciprocating speed of 5, 6.67, and 8.33 Hz. The morphologies, distributions of chemical element and phases of worn tracks were analyzed using a SEM, EDS, and XRD, respectively, and the profiles of worn tracks were analyzed using a VHX-700FC type super-deep three-dimensional microscopic system.

ANALYSIS AND DISCUSSION

Characterization of Cold Sprayed Al Coatings

Figure 1a shows the morphology of cold sprayed Al coating. The Al particles were impacted to the substrate surface by a high speed, the violent deformation occurred, which was distributed on the Al coating with the shape of flat strip. Figure 1b shows the morphology of cold sprayed Al coating cross-section with the thickness of $\sim 400 \mu\text{m}$. The Al coating was evenly distributed on the cross-section, there was no porosity or crack throughout the Al coating, the outlines of Al particles with the mutual combining were clear. The Al coating was closely combined with the substrate by the mechanical Mosaic way [20], there was a clear continuous cross-section without obvious defects. The XRD spectrum of Al coating is shown in Fig. 1c. The Al coating was composed of Al phase, no oxide was detected, indicating that the Al particles did not occur oxidation reaction in the cold spraying process.

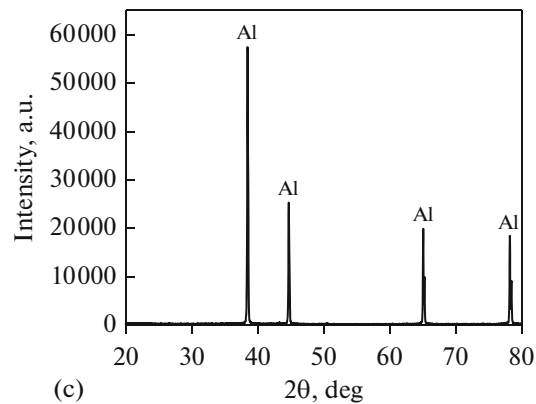
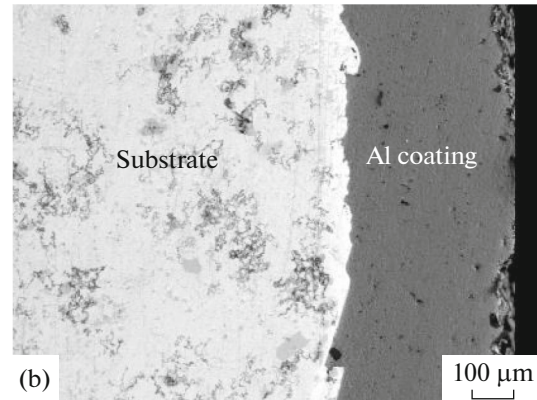
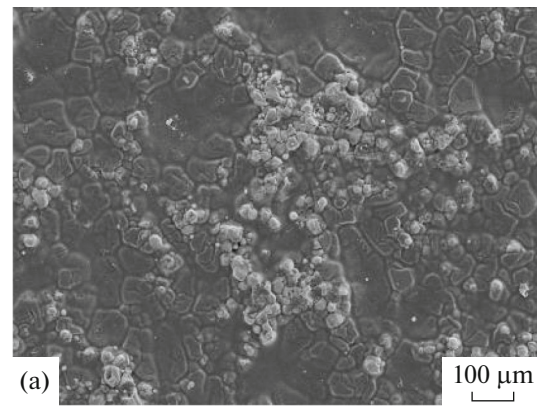


Fig. 1. Surface (a), cross-section (b) morphologies and XRD analysis (c) of cold sprayed Al coating.

COFs and Worn Profiles

The relations of COFs vs wear time at the different speeds are shown in Fig. 2a. The average COFs of Al coating at the reciprocating speeds of 5, 6.67, and 8.33 Hz were 0.29, 0.28, and 0.24, respectively, and the corresponding standard deviations were 1.10×10^{-1} , 7.70×10^{-2} , and 4.69×10^{-2} , respectively. The average and standard deviation of COFs of Al coating decreased with the increase of reciprocating speed, which tended to be smooth. The surface temperature of tribo-pair was small at the low reciprocating speed, the Al coating were difficult to cut and extrude, the

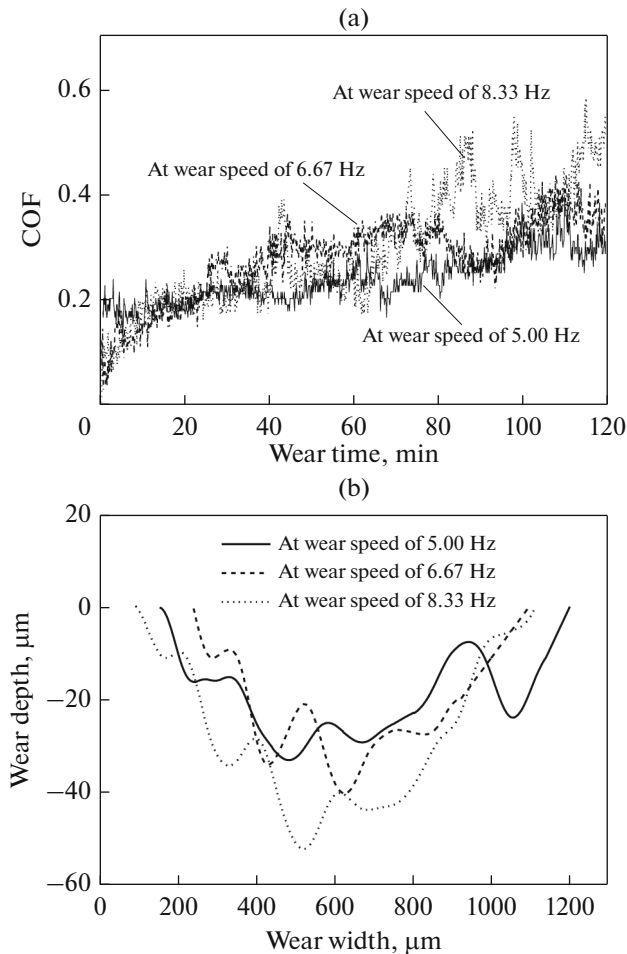


Fig. 2. COFs of cold sprayed Al coating vs wear time (a) and profiles of worn tracks (b) at different reciprocating speeds.

wear degree was not serious, this was because the high plastic deformation of Al coating came from the hindering effect among the micro-bumps [21]. As the wear test continuing, the contact area became large, the COFs of Al coating under the water lubrication decreased to some extent. From Fig. 2b, it can be seen that the wear rate increased with the increase of reciprocating speed, the unsmooth and irregular crack occurred on the Al coating. The wear rates of Al coating at the reciprocating speeds of 5, 6.67 and 8.33 Hz were 2.83×10^{-4} , 1.96×10^{-4} , and $2.36 \times 10^{-4} \text{ mm}^3/(\text{m N})$, respectively, and the corresponding depth of worn tracks was 35, 40, and 48 μm , respectively. This indicated that the wear rate of Al coating at the reciprocating speed of 6.67 Hz was the minimum, and its wear resistance was also the best among the three kinds of reciprocating speed.

Plane Scan Analysis of Worn Tracks

Figure 3a shows the plane scanned position of worn track at the reciprocating speed of 5 Hz. The plane

scan result is shown in Fig. 3b. The C and O appeared on the worn track, this was because the Al coating was covered by the sealing agent, which was not corroded in 3.5% NaCl solution. The Al formed the atom-rich zones on the worn track, this was because the sealing agent fell from the Al coating, as shown in Fig. 3c. The Na and Cl were very low, which were the residues came from 3.5% NaCl solution, as shown in Figs. 3d, 3e.

Figure 4a shows the plane scanned position of worn track at the reciprocating speed of 6.67 Hz. The plane scan result is shown in Fig. 4b. The Al on the worn track formed the atom-rich zones, which was smaller than that at the reciprocating speed of 5 Hz, as shown in Fig. 4c. The mass fraction of Al increased by 25.8% than that at the reciprocating speed of 5 Hz, this was because the Al debris was washed away by 3.5% NaCl solution. The Na and Cl were the residues of corrosion solution on the worn track, as shown in Figs. 4d, 4e.

Figure 5a shows the plane scanned position of worn track at the reciprocating speed of 6.67 Hz. The plane scan result is shown in Fig. 5b. The Al formed the atom-rich zones on the worn track, its mass fraction increased by 5.9% than that at the reciprocating speed of 6.67 Hz, indicating that the corrosion occurred on the Al coating, as shown in Fig. 5c. The remains of Na and Cl were adsorbed on the worn track, which were uniformly distributed, as shown in Figs. 5d, 5e.

From the above analyses, it can be seen that the Al contents increased with the increase of reciprocating speed, the O content was proportional to the corrosion degree, the corrosive wear resistance of Al coating at the reciprocating speed of 8.33 Hz was the best among the three kinds of speeds.

Wear Mechanism

Due to the interaction between the coating and the tribo-pair, a small amount of Al particles were fallen off from the coating and participated in the friction process [22], the exfoliated particles formed the furrows and micro-cuttings on the worn track at the reciprocating speed of 5 Hz, the wear mechanism was abrasive wear, as shown in Fig. 6a. Under the action of alternating stress, the deformation on the micro-volume of Al coating caused the cumulative damage, fatigue crack initiation and propagation, which produced the isolated granular or worn flakes on the worn track, the wear mechanism was fatigue wear, as shown in Fig. 6b. A large number of shedding and corrosion pits occurred on the Al coating, the wear mechanism was corrosive wear, as shown in Fig. 6c. From the above analyses, the wear mechanism of Al coating at the reciprocating speed of 5 Hz was abrasive wear, fatigue wear and corrosive wear. Under the actions of corrosion and wear, the spelled zones of Al coating increased, the corrosion pits were obviously found on the worn track, the wear mechanism was corrosive wear.

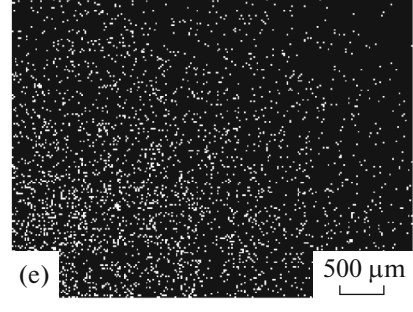
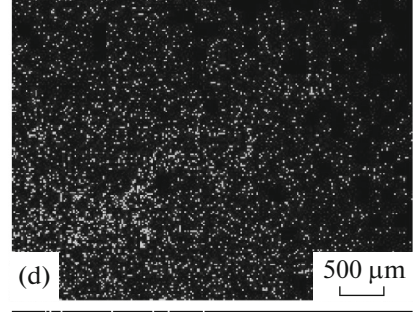
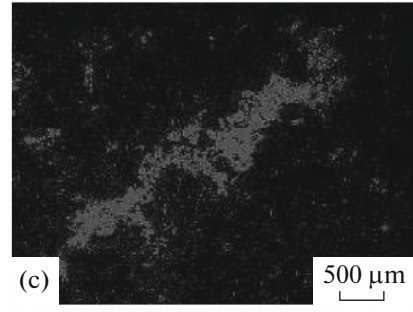
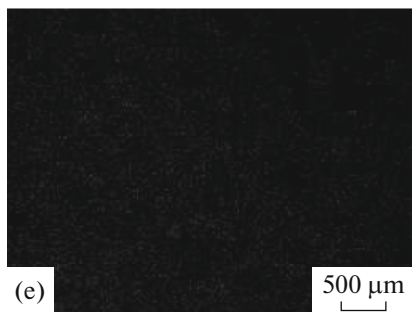
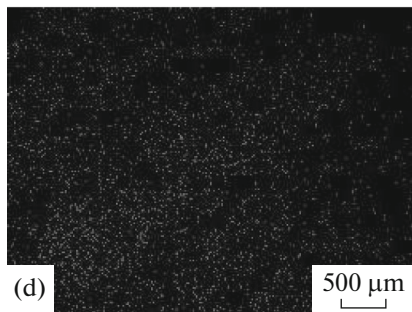
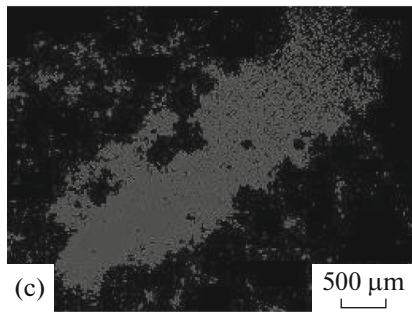
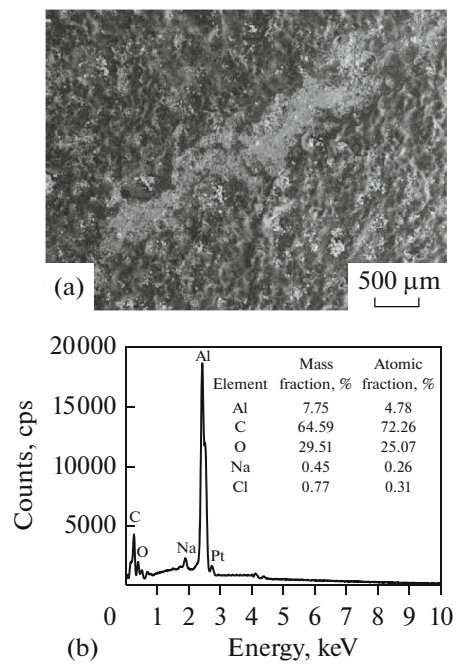
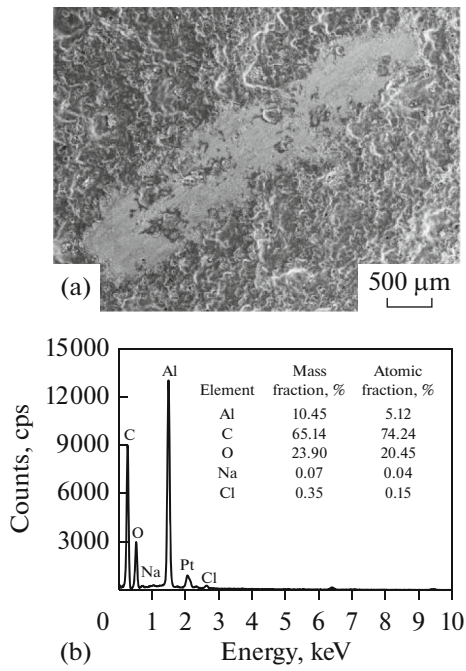


Fig. 3. Plane scan analysis of worn track at reciprocating speed of 5 Hz (under load of 1 N) (a) plane scanned position; (b) result of plane scan analysis; (c) Al content; (d) Na content; (e) Cl content.

Fig. 4. Plane scan analysis of worn track at reciprocating speed of 6.67 Hz (under load of 1 N) (a) plane scanned position; (b) result of plane scan analysis; (c) Al content; (d) Na content; (e) Cl content.

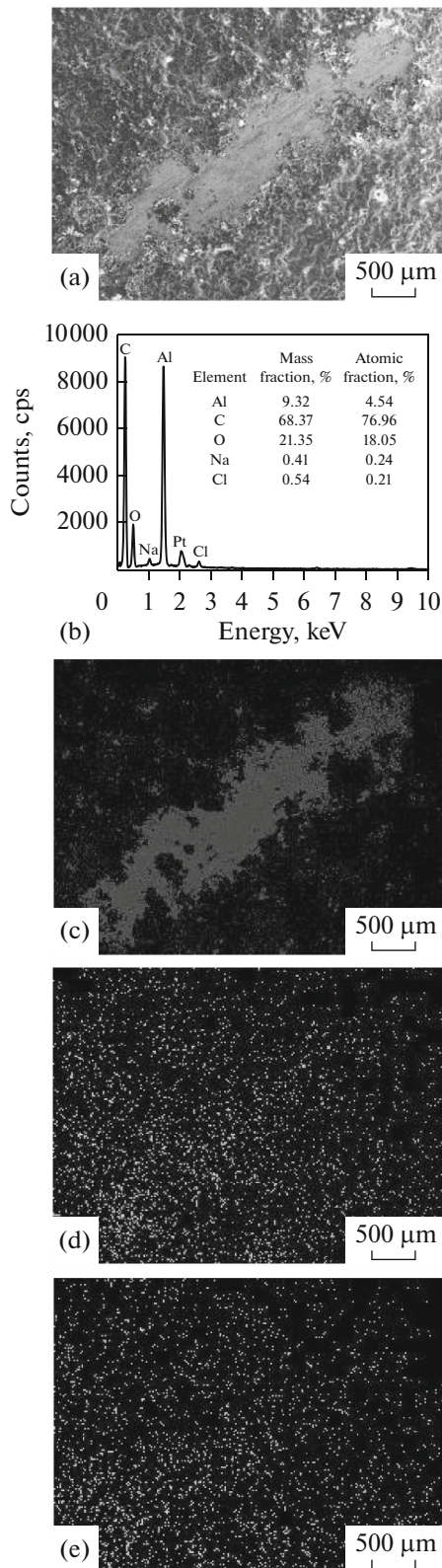


Fig. 5. Plane scan analysis of worn track at reciprocating speed of 8.33 Hz (under load of 1 N) (a) plane scanned position; (b) result of plane scan analysis; (c) Al content; (d) Na content; (e) Cl content.

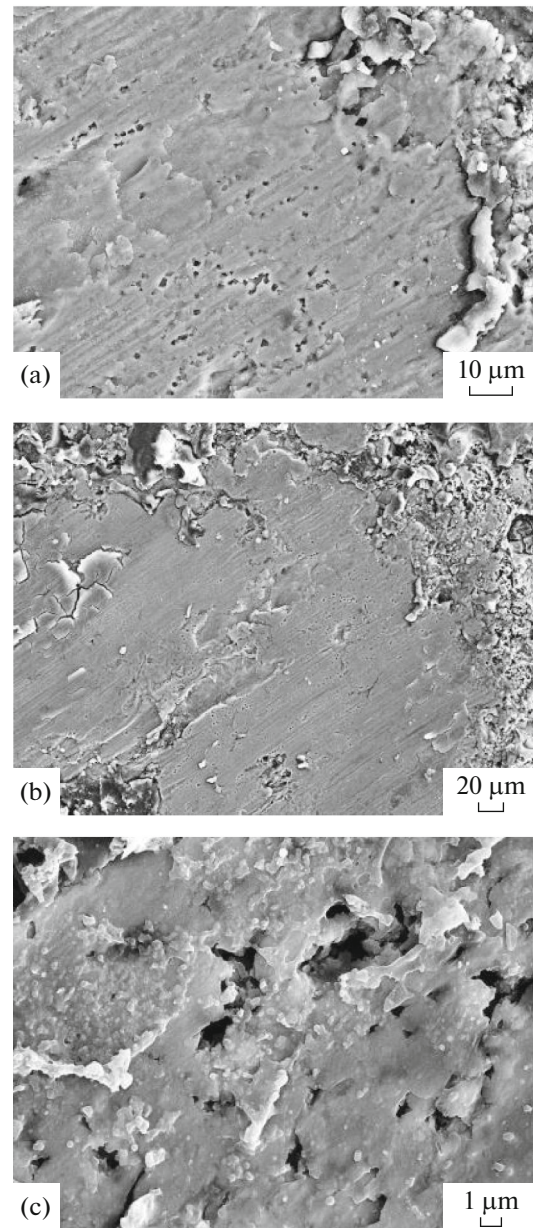


Fig. 6. Morphologies of worn track at reciprocating speed of 5 Hz (under g load of 1 N) (a) abrasive wear; (b) fatigue wear; (c) corrosion wear.

The striped furrows occurred on the worn track at the reciprocating speed of 6.67 Hz, the wear mechanism was abrasive wear, as shown in Fig. 7a. There were many flakes on the worn track, the wear mechanism was fatigue wear, as shown in Fig. 7b. The above reactions were slowed down, the intensity of corrosion pits on the worn track decreased, the depths of corrosion pits became small, the wear mechanism was corrosion wear, as shown in Fig. 7c. From the above analysis, the wear mechanism of Al coating at the reciprocating speed of 6.67 Hz was abrasive wear, fatigue wear and corrosive wear.

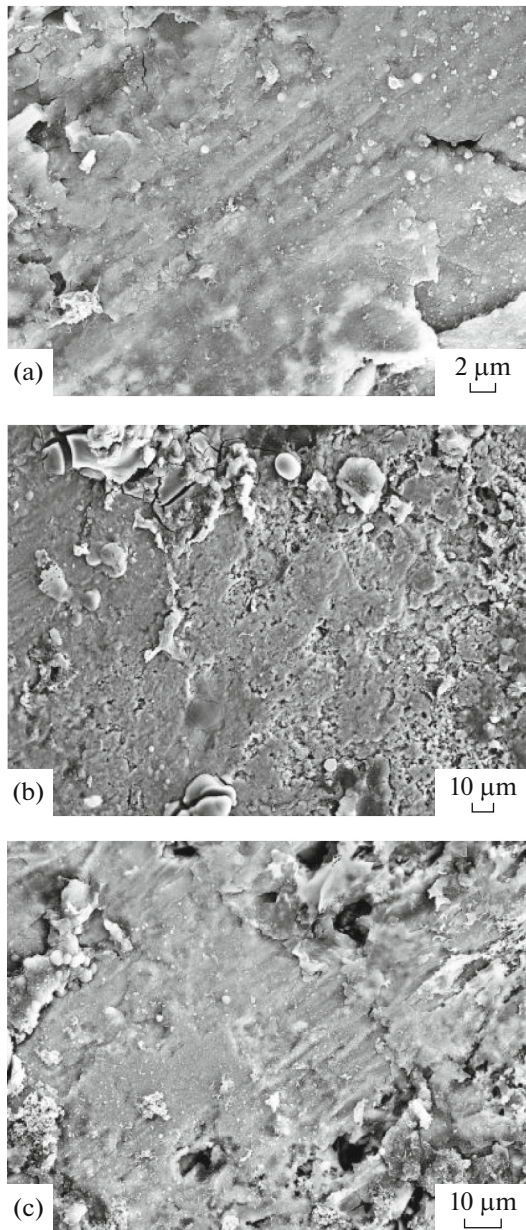


Fig. 7. Morphologies of worn track at reciprocating speed of 6.67 Hz (under load of 1 N) (a) abrasive wear; (b) fatigue wear; (c) corrosion wear.

The striped furrows also occurred at the reciprocating speed of 8.33 Hz, the wear mechanism was abrasive wear, as shown in Fig. 8a. A large number of small pieces appeared on the worn track, the Al coating was peeled off, the wear mechanism of was fatigue wear, as shown in Fig. 8b In the corrosive wear test, the Al coating generated chemical reactions in 3.5% NaCl solution and produced the corrosion products, the reactants were peeled off under the action of reciprocating load, which occurred the corrosive wear. The corrosion pits appeared on the worn track, the wear

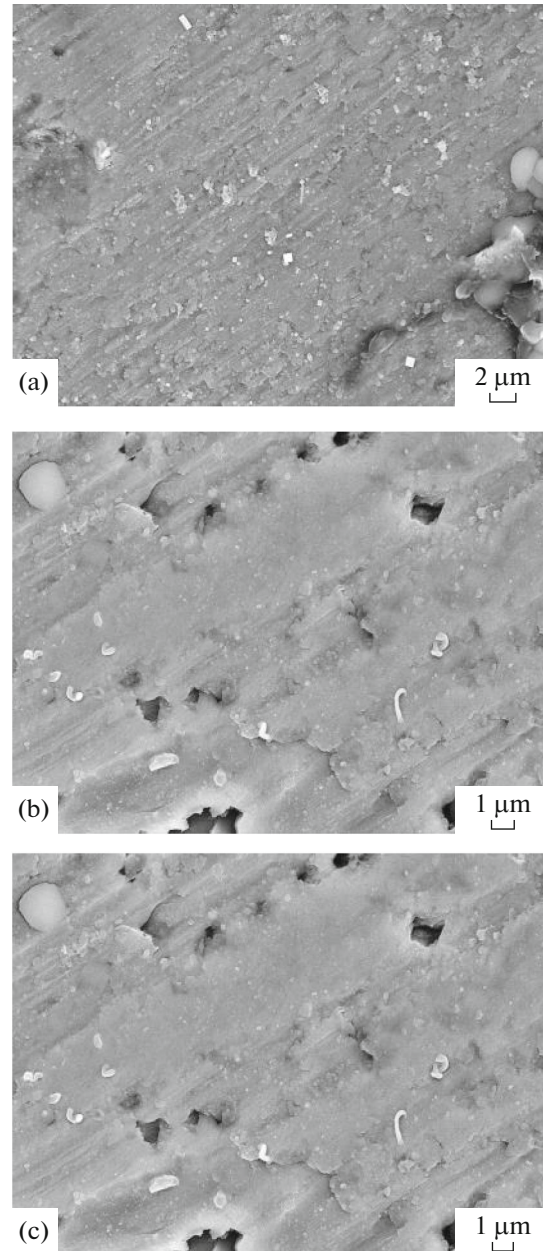


Fig. 8. Morphologies of worn track at reciprocating speed of 8.33 Hz (under load of 1 N) (a) abrasive wear; (b) fatigue wear; (c) corrosion wear.

mechanism was corrosive wear, as shown in Fig. 8c. As a result, the wear mechanism of Al coating at the reciprocating speed of 8.33 Hz was abrasive wear, fatigue wear and corrosive wear.

From the above analyses, the corrosion degree decreased with the increase of reciprocating speed, this was because the contact of Al coating on the worn track in 3.5% NaCl solution was not sufficient, the corrosion products were worn away. And the corrosive wear decreased with the increase of reciprocating speed, exacerbating its corrosive wear.

CONCLUSIONS

(1) The effects of reciprocating speed on corrosive wear behavior of cold-sprayed Al coating were investigated in 3.5% NaCl solution, which are shown as the following table. The average COFs of Al coating decrease with the increase of reciprocating speed, which is the lowest at the reciprocating speed of 8.33 Hz among the three kinds of speed. The wear resistance at the reciprocating speed of 6.67 Hz is the best among the three kinds of speed, which improves the corrosive wear of substrate on offshore platforms.

| Reciprocating speed, Hz | Average COF | Wear rate, mm ³ /(m N) |
|----------------------------|-------------|--------------------------------------|
| 5 | 0.29 | 2.83×10^{-4} |
| 6.67 | 0.28 | 1.96×10^{-4} |
| 8.33 | 0.24 | 2.36×10^{-4} |

(2) The wear mechanisms of Al coating are obtained from the worn morphologies, showing that those at the reciprocating speeds of 5, 6.67 and 8.33 Hz are primarily abrasive wear and fatigue wear, accompanied by corrosive wear at the reciprocating speeds of 5 and 6.67 Hz, and corrosive wear at the reciprocating speed of 8.33 Hz.

(3) The cold sprayed Al coating exhibits high corrosive wear resistance in 3.5% NaCl solution, which provides an effective protection on offshore platforms.

REFERENCES

1. Y. F. Jin, T. Y. Sheng, W. C. Kong, R. H. Zhang, W. C. Wang, and D. J. Kong, "Effects of strain rate on stress corrosion of S355 steel in 3.5% NaCl solutions," *J. Wuhan Univ. Technol., Mater. Sci. Ed.* **31**, 1381–1386 (2016).
2. J. Shen, F. S. Liu, H. J. Li, L. Xu, and B. C. Liang, "Assessment of the damages occurring between two adjacent measurements for an aging offshore platform," *Ocean Eng.* **109**, 372–380 (2015).
3. T. B. Matias, G. H. Asato, B. T. Ramasco, W. J. Botta, C. S. Kiminami and C. Bolfarini, "Processing and characterization of amorphous magnesium based alloy for application in biomedical implants," *J. Mater. Res. Technol.* **3**, 203–209 (2014).
4. S. L. Ngai, T. W. Ngai, F. Vogel, W. Story, G. B. Thompson, and L.N. Brewer, "Saltwater corrosion behavior of cold sprayed AA7075 aluminum alloy coatings," *Corros. Sci.* **130**, 231–240 (2018).
5. H. Z. Ye and J. F. Wang, "Preparation of aluminum coating on lexan by cold spray," *Mater. Lett.* **137**, 21–24 (2014).
6. A. Joshi and S. James, "Molecular dynamics simulation study of cold spray process," *J. Manufact. Process.* **33**, 136–143 (2018).
7. K. Ravi, T. Deplancke, K. Ogawa, J. Y. Cavallé, and O. Lame, "Understanding deposition mechanism in cold sprayed ultra high molecular weight polyethylene coatings on metals by isolated particle deposition method," *Addit. Manuf.* **21**, 191–200 (2018).
8. K. H. Ko, J. O. Choi, and H. Lee, "The interfacial restructuring to amorphous: A new adhesion mechanism of cold-sprayed coatings," *Mater. Lett.* **175**, 13–15 (2016).
9. K. H. Ko, J. O. Choi, and H. Lee, "Intermixing and interfacial morphology of cold-sprayed Al coatings on steel," *Mater. Lett.* **136**, 45–47 (2014).
10. Q. Wang, D. Qiu, Y. M. Xiong, N. Birbilis, and M. X. Zhang, "High resolution microstructure characterization of the interface between cold sprayed Al coating and Mg alloy substrate," *Appl. Surf. Sci.* **289**, 366–369 (2014).
11. J. Zhang and D. J. Kong, "Microstructures and salt spray corrosion behaviors of cold sprayed Al coatings on S355 steel in marine environment," *Surf. Rev. Lett.* **25**, 1850115 (2018).
12. B. Marzbanrad, H. Jahed and E. Toyserkani, "On the evolution of substrate's residual stress during cold spray process: A parametric study," *Mater. Design*, **138**, 90–102 (2018).
13. J. Zhang and D. J. Kong, "Effect of laser remelting on microstructure and immersion corrosion of cold-sprayed aluminum coating on S355 structural steel," *Opt. Laser Technol.* **106**, 348–356 (2018).
14. G. Benenati and R. Lupoi, "Development of a deposition strategy in cold spray for additive manufacturing to minimize residual stresses," *Proc. CIRP* **55**, 101–108 (2016).
15. D. Chen, Z. S. Li, H. L. Wu and D. L. Cong, "Study on corrosion resistance of cold sprayed pure aluminum coating," *Surf. Technol.* **45**, 174–179 (2016).
16. R. Morgan, P. Fox, J. Pattison, C. Sutcliffe, and W. O'Neill, "Analysis of cold gas dynamically sprayed aluminium deposits," *Mater. Lett.* **58**, 1317–1320 (2004).
17. A. Y. Churyumov, M. G. Khomutov, and A. A. Tsar'kov, "Study of the structure and mechanical properties of corrosion-resistant steel with a high concentration of boron at elevated temperatures," *Phys. Met. Metallogr.* **115**, 809–813 (2014).
18. X. M. Bai, J. Q. Tang, J. M. Gong, and X. L. Lü, "Corrosion performance of Al–Al₂O₃ cold sprayed coatings on mild carbon steel pipe under thermal insulation," *Chin. J. Chem. Eng.* **25**, 533–539 (2017).
19. H. Assadi, H. Kreye, F. Gärtner, and T. Klassen, "Cold spraying—A materials perspective," *Acta Mater.* **116**, 382–407 (2016).
20. S. Kumar and A. A. Rao, "Influence of coating defects on the corrosion behavior of cold sprayed refractory metals," *Appl. Surf. Sci.* **396**, 760–773 (2017).
21. Y. Zhang, X. Yin, J. Wang, and F. Yan, "Influence of microstructure evolution on tribocorrosion of 304SS in artificial seawater," *Corros. Sci.* **88**, 423–433 (2014).
22. L. G., Korshunov and N. L. Chernenko, "Effect of aluminum on the structural transitions and the wear resistance of hadfield steel under friction," *Phys. Met. Metallogr.* **117**, 700–706 (2018).